

- D.-G. Oei, *J. Appl. Electrochem.* **12**, 87 (1982); *ibid.* **15**, 619 (1985).
5. A. M. Posner, *Fuel* **24**, 330 (1955).
 6. J. M. Matsen, *Adv. Chem. Ser.* **64**, 277 (1967).
 7. Parr Instruments, Moline, IL.
 8. The Pt black (Aesar, fuel cell grade) was heated (185°C) under vacuum (0.03 torr) for 30 min before use. The $\text{Fe}_2(\text{SO}_4)_3$, H_2SO_4 (both Aesar, puratronic grade), and CH_4 (Matheson, ultrahigh purity) were used as received. Very high purity was required for the reagents to avoid catalyst poisoning. The water was deionized and doubly distilled. All solutions were deoxygenated, and the reactions were set up under 1 atm of Ar.
 9. The dispersion of the Pt black (6.99%) was determined by titration with pulses of H_2 and O_2 (14). The rate of oxidation of CH_4 by Fe(III) was determined by bleeding aliquots of the reaction mixture through the needle valve and titrating them with Ce(IV) . The rates obtained were approximate because the volume of solution decreased with each aliquot removed, which changed the mass transport properties of the reaction. We measured the amount of CO_2 by trapping it with a standard solution of Ba(OH)_2 (0.1 M) in water and then titrating the unreacted Ba(OH)_2 with a standard solution of HCl (0.1 M) in water. The amounts of Fe(II) and of CO_2 agreed within $\pm 10\%$. No other products were detected in either the reaction mixture (analyzed by high-performance liquid chromatography with a Bio-Rad AMINEX column) or in the atmosphere of the bomb (analyzed by Fourier transform infrared spectroscopy and by gas chromatography mass spectroscopy).
 10. The density and surface area of WDF graphite felt (Union Carbide) are $8.49 \times 10^{-2} \text{ g/cm}^3$ and $0.5 \text{ m}^2/\text{g}$, respectively. We did not measure the surface area or the density of WDF graphite felt after it was treated with boiling, concentrated HNO_3 . The geometric volumes of the electrodes (measured with a ruler) were used to calculate current densities. Because the electrodes are composed of thick porous felts, current densities are appropriately reported as volume densities (for example, milliamperes per cubic centimeter). The electrode chambers of the fuel cell were 3 cm in diameter and 5.5 cm deep. Each chamber contained a saturated calomel reference electrode. The chambers were separated by a Nafion 117 proton exchange membrane. The anode and cathode were rectangles of graphite felt that were 2 cm wide, 3 cm high, and 0.5 cm deep. The projected area of the anode and cathode on the Nafion membrane was 6 cm^2 . The current collectors were Pt wires (0.5 mm in diameter and $\sim 4 \text{ cm}$ long) that were threaded through the graphite felt. Graphite rods can also be used as current collectors but with higher polarizations.
 11. D.-G. Oei, *J. Appl. Electrochem.* **12**, 41 (1982).
 12. S. H. Bergens and G. M. Whitesides, unpublished results.
 13. P. Münster and H. Grabke, *J. Catal.* **72**, 279 (1981).
 14. L. Carballo, C. Serrano, E. E. Wolf, J. J. Carberry, *ibid.* **52**, 507 (1978).
 15. A. J. Bard, R. Parsons, J. Jordan, *Standard Potentials in Aqueous Solution* (Dekker, New York, 1985). We were unable to experimentally or theoretically determine the formal potentials of $\text{O}_2\text{-H}_2\text{O}$ and of $\text{CO}_2\text{-CH}_4$. $E_{\text{loss O}_2}$ and $E_{\text{loss CH}_4}$ therefore only approximate the differences in formal potentials between $\text{O}_2\text{-H}_2\text{O}$ and $\text{VO}_2\text{VO}^{2+}$ and between $\text{CO}_2\text{-CH}_4$ and Fe(III)-Fe(II) .
 16. This work was supported in part by the Advanced Research Projects Agency. S.H.B. thanks the National Engineering and Research Council of Canada for a postdoctoral fellowship. G.T.R.P. thanks the National Science Foundation for a postdoctoral fellowship. We thank both M. S. Wrighton and D. Maricle for useful discussions. R. Porcelli first pointed out the König patent to G.M.W.

25 March 1994; accepted 1 July 1994

A Spectroscopic Measurement of the Coronal Density of Procyon

J. H. M. M. Schmitt,* B. M. Haisch, J. J. Drake

One of the open key issues in the astrophysics of stellar coronae is the determination of their spatial structure and density. From almost all previous measurements, one can infer merely the presence of a corona, which for the most energetic stellar coronae may exceed the solar x-ray output by as much as five orders of magnitude, but no information can be obtained on the densities and hence volumes and sizes of the hot x-ray emitting material. A direct spectroscopic measurement of the coronal density was obtained for the star Procyon with the spectrometer on board the Extreme Ultraviolet Explorer satellite; the ratio of two Fe XIV lines at 211.32 and 264.79 angstroms was used to determine a density of $\sim 4 \times 10^9$ to 7×10^9 electrons per cubic centimeter, which is a factor of 2 to 3 higher than typical solar active region densities. From this value, we estimate that ~ 6 percent of the stellar surface is covered with $\sim 7 \times 10^4$ coronal loops.

The x-ray images of the sun obtained from Skylab (1), the Normal Incidence X-ray Telescope (NIXT) (2), and Yohkoh (3) have revealed an extremely complex structure in the solar corona. This structuring is

J. H. M. M. Schmitt, Max-Planck-Institut für Extraterrestrische Physik, 85740 Garching, Germany.
B. M. Haisch, Max-Planck-Institut für Extraterrestrische Physik, 85740 Garching, Germany, and Lockheed Solar and Astrophysics Laboratory, Division 91-30, Building 252, 3251 Hanover Street, Palo Alto, CA 94304, USA.
J. J. Drake, Center for Extreme Ultraviolet Astrophysics, University of California, Berkeley, CA 94720, USA.

*To whom correspondence should be addressed.

the result of the confinement of the coronal plasma in magnetic loops, and in fact, most of the solar x-ray emission comes from a relatively small number of such loops spatially concentrated in active regions. Observations with the Einstein Observatory (4) and Roentgen Satellite (ROSAT) (5) telescopes have revealed x-ray emission from all classes of late-type stars except evolved K and M stars that are beyond the coronal dividing line (6). Does such emission originate in stellar analogs of solar active regions?

Stars cannot be spatially resolved, and thus, their coronal filling factors (that is, the fraction of their coronal volumes that emit x-rays) cannot be directly measured. Even in the rare cases of eclipsing binaries from which sizes of coronal structures can be inferred (7), it is impossible to distinguish between a diffusely filled structure and one in which the plasma is threaded through only a fraction of the volume. Heretofore, it has been impossible to determine whether, on a given star, coronal emission originates in rather compact high-density regions or in extended tenuous low-density regions because only the product of the square of the electron density and the volume (that is, the volume emission measure, $\text{VEM} = n^2V$) could be determined from broadband flux or low-spectral resolution observations hitherto available. This dependence on n^2 arises from the dominant cooling process, that is, the excitation of ions by thermal electrons followed by radiative decay; because most of the gas is hydrogen, which is fully ionized at coronal temperatures, $n = 0.85n_e$, where n_e is the electron density. Consequently, spectroscopic measurements of n_e become of utmost importance because they can, in principle, be obtained for any coronal star, and from the VEM, which is directly derivable from the measured flux, the volume can be derived. Linear size scales of the x-ray emitting regions can then be determined on the basis of models of magnetic loops developed for the sun.

The star Procyon is a nearby astrometric binary consisting of a slightly evolved F5 IV-V star with a cool white dwarf companion. The x-ray emission from Procyon was first discovered with the Einstein Observatory's Imaging Proportional Counter (IPC) (8), which measured a luminosity of $L_x \approx 10^{28} \text{ ergs s}^{-1}$, about the same L_x as the sun at solar maximum. All of the observed x-ray emission was attributed to Procyon A (the F-type star), and the coronal temperature was found to be rather low ($T_{\text{cor}} \sim 10^{6.2} \text{ K}$) when compared with other stars with higher x-ray luminosity (9). On the other hand, because Procyon is slightly larger than the sun (radius $R_* \approx 1.9 R_\odot$, where R_\odot is the radius of the sun), the x-ray emission expressed as a surface flux is rather similar to that of the quiet sun, for which such a low T_{cor} would be appropriate.

Procyon has also been investigated with both the International Ultraviolet Explorer (IUE) and the European X-ray Observatory Satellite (EXOSAT). An extensive study of Procyon with IUE yielded the detection of a large number of chromospheric and transition-region lines (10); the ultraviolet line with the highest formation temperature is the N V line at 1240 \AA with $T \sim 10^{5.2} \text{ K}$. The spectrum of Procyon obtained with the

transmission grating spectrometer (TGS) on board the EXOSAT satellite covered the wavelength range from 10 to 200 Å with a spectral resolution of ~ 3 Å. The EXOSAT TGS count spectrum [see figure 4 in (11)] clearly shows lines or line complexes, but no attempt was made to identify individual lines (11); rather, the spectrum was interpreted with a spectral synthesis code (12).

Under a National Aeronautics and Space Administration (NASA) Guest Observer Program, we were granted time to observe Procyon with the Extreme Ultraviolet Explorer (EUVE) grating spectrometer (13). Briefly, the EUVE slitless spectrometer covers the wavelength range from 70 to 750 Å in three bands (known as the short, medium, and long wavelength channels; hereafter SW, MW, and LW, respectively), with an effective area of typically 0.5 to 1.0 cm² and a spectral resolution between 0.5 and 2 Å. The observations presented here were taken between 11 January 1993, UT 22:19, and 15 January 1993, UT 00:28, with a total integration time of about 96,000 s.

Because of the large number of known lines in the solar EUV (14–17), identification of most of the observed spectral features was straightforward. However, some of the identifications should perhaps be considered preliminary because the known systematic errors in the spectrometer wavelength calibration can be quite large (up to 1 Å in the MW channel, according to the EUVE Guest Observers handbook). Because such systematic errors are a slowly varying function of wavelength, line identification can proceed by bootstrapping from the reasonably secure identifications of prominent spectral features. We have done this and point out in Fig. 1 the series of strong iron lines between ~ 170 and 200 Å (well known from solar EUV spectra), the helium lines at 256 and 304 Å, and the Fe XV line at 284.15 Å but defer a detailed discussion of the full EUVE spectrum to elsewhere.

The solar EUV spectral range contains a multitude of lines that can be used for spectroscopic density diagnostics (18). The stellar difficulties are twofold: (i) In contrast to the sun, the presently available instrumentation and the relative weakness of stellar spectra permit detection of only the stronger lines, and (ii) the spectral resolution is in many cases not high enough to ensure that the detected lines are unblended. As a consequence, many of the density-sensitive line ratios used in solar observations cannot be used unambiguously for our stellar observations.

We have identified a density-sensitive line pair of the Fe XIV ion in the Procyon spectrum that is both reasonably strong and unblended. A detailed theoretical study of Fe XIV (19) shows that the three strongest

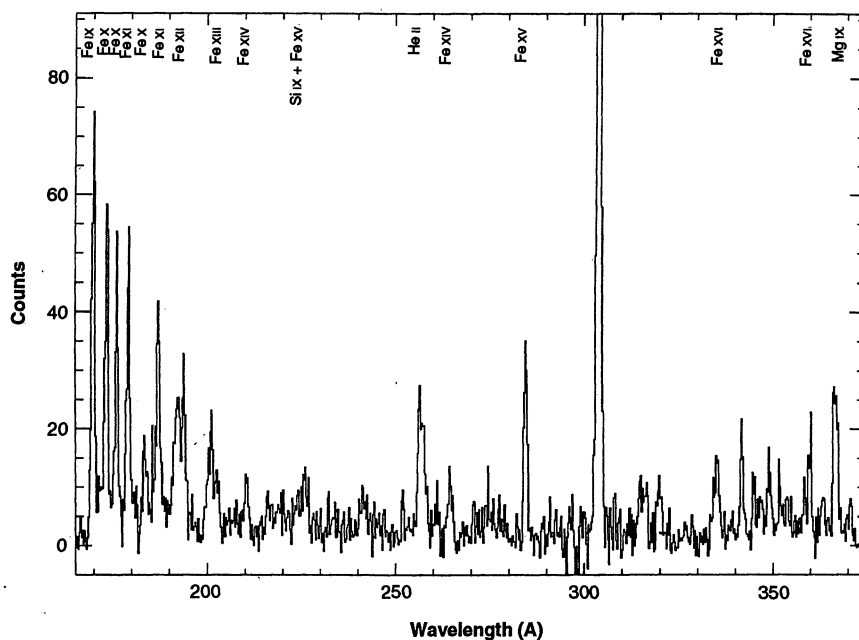


Fig. 1. The EUVE MW spectrum for Procyon; the strongest line features have been identified with the dominant ion responsible for the observed emission. Special attention was devoted to the spectral extraction because the dispersed spectra appear slightly curved along the dispersion direction in the spectrometer detector images. An optimal width of the spectrum was determined perpendicular to the dispersion direction for each of the three spectrometer channels; the centroid of each spectrum was then obtained along the dispersion direction, and a fifth-order polynomial was fit to these data. The final extractions of the spectra were then made with the optimal widths along a dispersion direction defined by these polynomial fits. The extracted and wavelength-calibrated spectra were binned over four pixels (corresponding to a spectral resolution of 1 Å in the MW channel).

lines of Fe XIV in a low-density environment are the $^2P\text{-}^2D$ transition at wavelength $\lambda = 211.32$ Å, the $^2S\text{-}^2P$ transition at 274.20 Å, and the $^2P\text{-}^2P$ transition at 264.79 Å; with increasing density, the first two lines decrease in intensity, whereas the third increases. At higher densities, another line from the $^2D\text{-}^2P$ transition at 219.12 Å appears, which in fact becomes the strongest Fe XIV line at densities in excess of 10^{10} cm⁻³ [see figure 1 in (19)]. These theoretical expectations are borne out by high-resolution solar EUV spectra. For example, in a full-disk quiet sun spectrum taken on 4 April 1969 (16), the lines at wavelengths 211.32, 264.79, and 274.20 Å are the strongest Fe XIV lines (in this order), whereas the line at 219.12 Å is detected but weak; on the other hand, in a flare spectrum taken on 17 December 1973 (20), the line at 219.12 Å is more intense than the one at 211.32 Å.

A comparison with various x-ray line lists (11, 14–16) shows that the Fe XIV line at 274.20 Å is close to some stronger Si VII and Si X lines, and the Fe XIV line at 219.12 Å is close to a few lines of iron in various ionization stages and is comparable in strength. On the other hand, the Fe XIV lines at 211.32 and 264.79 Å are relatively unaffected by blends. The only potentially significant line in the vicinity of 264.79 Å is the $^4S\text{-}^4P$ transition in S X at 264.24 Å. In the vicinity of 211.32 Å, there is only the weak Fe XII $^2D\text{-}^2P$ transition

at 210.46 Å and another Fe XII $^2D\text{-}^2P$ transition at 211.74 Å.

In Table 1, we list the various Fe XIV lines considered, their solar and EUVE measured wavelengths, their fitted amplitudes and errors (in counts), and the effective area of the spectrometer at each wavelength. The line amplitudes were obtained with the use of a maximum likelihood technique to fit one or more Gaussian profiles to the observed count distribution; in the fit process, we kept the relative wavelengths of the lines with respect to each other fixed and varied the overall wavelengths as well as the amplitudes of all the lines. As a "spectral line template," we used the strong He line at 304 Å, which can be well fit by this technique.

The line at 264.79 Å is not well fit by a single Gaussian line profile; there is an excess at shorter wavelengths, which can be matched by introducing a second line, which we take to be the S X line at 264.24 Å, mentioned above. Under quiet solar conditions, another S X transition at 259.49 Å is observed at almost the same intensity as the S X line at 264.24 Å. In our Procyon spectrum, we found absolutely no evidence for such a line at 259.49 Å and obtained an upper limit of <20 counts for a line at that position; we infer that any S X contribution to the Fe XIV line at 264.79 Å should then also be <20 counts, and we believe this

estimate to be conservative because the value in Table 1 for the 264.79 Å line refers to the fitted number of counts under the line profile (and not the actual measured number of counts).

At the positions of the Fe XIV lines at 219.12 and 220.08 Å, there is a clear detection of a stellar signal, but we cannot resolve the lines. The numbers in Table 1 are derived from a fit of two Gaussian lines at the respective line positions and should therefore be treated with some caution. The same applies to the lines at 270.52 and 274.03 Å. Finally, at the Fe XIV line at 289.16 Å, we find only a statistically insignificant feature and therefore cite an upper limit only.

From the point of view of plasma density diagnostics, the most interesting lines are those at 211.32, 264.79, and 219.12 Å. The ratio between the first two lines varies by a factor of 3 between low and high density, and the mere presence of a line at 219.12 Å indicates high density. We compute a line ratio (in energy units, corrected for telescope effective area) of 0.84 ± 0.12 for the lines at 264.79 and 211.32 Å; if we (generously) allow for a contamination of 20 counts in the 264.79 Å line, we obtain a minimum ratio >0.69 .

Before converting line ratios to n_e , we need to consider differential absorption by the intervening interstellar hydrogen column density. For the line-of-sight toward Procyon, values ranging from 3×10^{17} to $1.5 \times 10^{18} \text{ cm}^{-2}$ have been reported (21, 22); no information is available on the ionization state of helium along this line-of-sight. The corrected (de-reddened) ratio between the 264.79 and 211.32 Å lines could thus be larger than the measured ratio by 5 to 30%.

The measured 264.79/211.32 line strength ratio of 0.84 ± 0.12 corresponds to $\log n_e = 9.7 \pm 0.15$, if the calculations by Blaha are used [see table VII in (19)]. We have compared this conversion between line ratio and density to that obtained from more recent calculations (23, 24) and found the two conversions compatible to within the observational errors. The lower limit to this line strength ratio, allowing for maximum contamination of the line at

264.79 Å by the possible S X blend, corresponds to $\log n_e > 9.4$. Now, the higher of the above-mentioned hydrogen column densities would imply a 30% correction to the 264.79/211.32 line ratio, leading to $\log n_e = 10.0 \pm 0.15$. As stated above, the mere presence of the line at 219.12 Å indicates a high pressure. Even though the statistics are extremely poor, we can formally find a 219.12/211.32 ratio of 0.50, implying $\log n_e = 9.55$, but this determination has an extremely large error. All other Fe XIV line ratios also have large errors and therefore provide no new information, but they do appear to be consistent with the densities derived above.

We conclude that Procyon's average coronal density is at least as large as $\log n_e > 9.4$, with the most likely values lying between $\log n_e = 9.55$ and 9.85. To our knowledge, this is the first direct measurement of the coronal density in another solar-like star. In this context, we wish to note that coronal density estimates for the star Capella have been derived from Fe XXI lines observed also with the EUVE satellite (26); however, Capella is not a solar-like star either from the optical or from the x-ray point of view, and further, three line ratios from the same ion resulted in density values that differ by almost a factor of 40, whereas in our measurements, all line ratios considered are consistent. On the sun, the Fe XIV 264.79/211.32 line ratio varies between 0.49 and 0.63, definitely below our values for Procyon. Hence, the coronal density of Procyon must be somewhat larger than that of typical solar active region densities (25), above $\log n_e = 9.3$. Combining this density measurement with the characteristic line-formation temperature of $\log T_{\text{cor}} = 6.3$, we derive a coronal pressure of ≈ 2 dyne.

From the measured line flux of 3.2×10^{-3} photons $\text{cm}^{-2} \text{ s}^{-1}$ in the Fe XIV line at 264.79 Å and the Mewe *et al.* (12) line power of $10^{-23.94} \text{ erg cm}^2 \text{ s}^{-1}$ [corrected by a factor of 1.3 for density (see their table Vib)], we can determine the total emission measure (assuming all the material is at $\log T = 6.3$) of $\text{VEM} = 2.3 \times 10^{50} \text{ cm}^{-3}$. Then; using $n_e = 5 \times 10^9 \text{ cm}^{-3}$ from our spectroscopic density measurement, we find an emitting volume of $V \approx 9 \times 10^{30} \text{ cm}^3$

(for the visible hemisphere of the star). If this emission were uniformly distributed over the visible hemisphere of Procyon, the height would be $h = V/2\pi R_*^2 = 8 \times 10^7 \text{ cm}$. The Rosner, Tucker, and Vaiana (27) scaling law for solar coronal loops predicts a loop length $L = 1.3 \times 10^9 \text{ cm}$. If we assume that L is the true scale height for the emission, the filling factor would thus be on the order of 6%. To estimate the number of loops across the entire surface, we let α represent the aspect ratio (width to length) of coronal loops so that $2\pi N\alpha^2 L^3 \approx V$. We find that for $\alpha \approx 0.1$, there are on the order of $N \approx 7 \times 10^4$ loops distributed over about 6% of the surface of Procyon. These loops must be distributed fairly homogeneously over Procyon's surface to be consistent with the lack of any measurable variability in its coronal emission (28).

REFERENCES

1. M. Z. Zombeck *et al.*, *Astrophys. J. Suppl.* **38**, 69 (1979).
2. L. Golub *et al.*, *Nature* **344**, 842 (1990).
3. L. Acton *et al.*, *Science* **258**, 618 (1992).
4. G. S. Vaiana *et al.*, *Astrophys. J.* **245**, 163 (1981).
5. J. H. M. M. Schmitt, in *Cool Stars, Stellar Systems, and the Sun: Seventh Cambridge Workshop*, M. S. Giampapa and J. A. Bookbinder, Eds. (ASP Conference Series 26, Astronomical Society of the Pacific, San Francisco, 1992), p. 83.
6. B. Haisch, J. H. M. M. Schmitt, A. C. Fabian, *Nature* **360**, 239 (1994).
7. J. H. M. M. Schmitt and M. Kürster, *Science* **262**, 215 (1993).
8. J. H. M. M. Schmitt, F. R. Harnden Jr., G. Peres, R. Rosner, S. Serio, *Astrophys. J.* **288**, 751 (1985).
9. J. H. M. M. Schmitt *et al.*, *ibid.* **365**, 307 (1990).
10. A. Brown and C. Jordan, *Mon. Not. R. Astron. Soc.* **196**, 757 (1981).
11. J. R. Lemen, R. Mewe, C. J. Schrijver, A. Fludra, *Astrophys. J.* **341**, 474 (1989).
12. R. Mewe, E. H. B. M. Gronenschild, G. H. J. van den Oord, *Astron. Astrophys. Suppl. Ser.* **62**, 197 (1985).
13. S. Bowyer and R. F. Malina, in *Extreme Ultraviolet Astronomy*, R. F. Malina and S. Bowyer, Eds. (Pergamon, Tarrytown, NY, 1991), pp. 379–408.
14. K. P. Dere, *Astrophys. J.* **221**, 1062 (1978).
15. W. E. Behring, L. Cohen, U. Feldman, G. A. Doschek, *ibid.* **203**, 521 (1976).
16. M. Malinovsky and L. Heroux, *ibid.* **181**, 1009 (1973).
17. U. Feldman, P. Mandelbaum, J. F. Seely, G. A. Doschek, H. Gursky, *Astrophys. J. Suppl.* **81**, 387 (1992).
18. G. A. Doschek, in (13), pp. 94–112.
19. M. Blaha, *Sol. Phys.* **17**, 99 (1971).
20. K. P. Dere, H. E. Mason, K. G. Widing, A. K. Bhatia, *Astrophys. J. Suppl.* **40**, 341 (1979).
21. R. G. Evans, C. Jordan, R. Wilson, *Mon. Not. R. Astron. Soc.* **172**, 585 (1975).
22. J. Murthy *et al.*, *Astrophys. J.* **315**, 675 (1987).
23. F. P. Keenan, P. L. Dufton, M. B. Boylan, A. E. Kingston, K. G. Widing, *ibid.* **373**, 695 (1991).
24. A. K. Bhatia, S. O. Kastner, F. P. Keenan, E. S. Conlon, A. G. Widing, *ibid.* **427**, 497 (1994).
25. R. J. Bray, L. E. Cram, C. J. Durrant, R. E. Loughhead, *Plasma Loops in the Solar Corona* (Cambridge Univ. Press, Cambridge, 1991).
26. A. K. Dupree, N. S. Brickhouse, G. A. Doschek, J. C. Green, J. C. Raymond, *Astrophys. J. Lett.* **418**, 41 (1993).
27. R. Rosner, W. H. Tucker, G. S. Vaiana, *Astrophys. J.* **220**, 643 (1978).
28. B. M. Haisch and J. H. M. M. Schmitt, *ibid.* **426**, 716 (1994).

8 April 1994; accepted 5 July 1994

Table 1. The Fe XIV lines detected in the EUVE Procyon spectrum.

Transition lower-upper	Wavelength		Counts	Effective area (cm ²)	Remarks
	Å _{obs}	Å _{solar}			
3s ² 3p ² P _{1/2} -3s ² 3d ² D _{3/2}	210.45	211.32	115±11	0.39	Unblended
3s ² 3p ² P _{3/2} -3s ² 3d ² D _{5/2}	219.0	219.12	59± 9	0.38	Blended
3s ² 3p ² P _{3/2} -3s ² 3d ² D _{3/2}		220.08	51± 8	0.38	Blended
3s ² 3p ² P _{3/2} -3s3p ² P _{3/2}	264.50	264.79	109±10	0.35	Unblended
3s ² 3p ² P _{1/2} -3s3p ² P _{3/2}	270.59	270.52	43± 8	0.35	Blended
3s ² 3p ² P _{1/2} -3s3p ² S _{1/2}	274.50	274.20	70± 9	0.36	Blended
3s ² 3p ² P _{3/2} -3s3p ² S _{1/2}		289.16	<24	0.38	